Progress In Electromagnetics Research C, Vol. 128, 247–261, 2023

Compact Metamaterial Loaded Wideband Monopole Antenna for Wireless Applications

Shaik A. Khadar* **and Sudhakar Sahu**

Abstract—A compact metamaterial-loaded wideband monopole antenna is reported in this paper for wireless applications. Initially, a monopole antenna with a single stub was designed to resonate at 4 GHz. Still, it suffers from low gain, so to enhance the antenna parameters, a metamaterial unit cell was considered along the feed line and ground plane. Double split ring resonator (DSRR) is a modified unit cell of a typical split ring resonator (SRR) designed to achieve a good coupling effect. The dimensions of the proposed DSRR unit cell are $0.17\lambda_0 \times 0.17\lambda_0$, where λ_0 is the free space wavelength at 4 GHz. It achieved an impedance bandwidth (-10 dB) in the frequency range of 3.38 GHz to 4.08 GHz & 4.64 GHz to 5.2 GHz, having a 19.49% bandwidth in the 1st band and 11.7% bandwidth in the 2nd band. A wideband was achieved in the frequency range of 3.39 GHz to 5.13 GHz with 47.9% bandwidth when the number of stubs was increased to four. A maximum gain of 3.3 dBi was attained with bidirectional radiation in the E-plane, and it was omnidirectional in the H-plane. By increasing the number of stubs, two resonant modes were merged, making it wideband and suitable for WLAN applications like Wi-Fi & WiMAX & Satellite Communications.

1. INTRODUCTION

Planar microstrip antenna plays an essential role in modern wireless communication systems. It is easy to fabricate with radiating elements on one side and a ground plane on the other side of the substrate. Still, it has narrow bandwidth, low gain, and poor radiation efficiency. Designing compact, low-cost, high-gain, multiband, and wideband antennas is a challenging task faced by researchers. High gain [1] can be achieved using antenna arrays. In contrast, multiband structures can be achieved either by introducing slots [2, 10] in the patches, truncating the ground plane, or placing shorting pins [3] between the patch and ground plane. However, these antennas cannot provide miniaturization. Many researchers have recently incorporated metamaterials into planar microstrip antennas to enhance antenna parameters.

An artificial homogeneous material with negative permittivity and permeability is called Metamaterial Unit Cell. Metamaterials are also called Left-Handed Materials because the magnetic field vector, electric field vector, and phase propagation vector form a left-handed triplet. Due to the novel metamaterial properties, they found many applications, such as absorbing, blocking, and cloaking at radio and microwave frequencies. In [4], Samson Daniel et al. proposed a monopole antenna with an inverted U-shaped slot and a partial ground plane. Composite slip ring resonator (CSRR) was introduced inside the monopole antenna to resonate at 2.1/3.45/5.43 GHz with a bandwidth of 80/110/670 MHz, making it suitable for applications such as universal mobile telecommunication system (UTMS), WiMAX, and WLAN. A triple band antenna inspired by a metamaterial unit cell was proposed in [5] for WCDMA, Bluetooth, WLAN, and WiMAX applications, where a triangle-shaped metamaterial unit cell along a microstrip feed line was detached on one side of the substrate with a defected ground plane on the other side and achieved resonance at 1.9/2.45/5 GHz with a bandwidth

Received 1 December 2022, Accepted 3 January 2023, Scheduled 17 January 2023
* Corresponding author: Shaik Abdul Khadar (abdulkhader.shaik08@gmail.com).
The authors are with the School of Electronics Engineering, KIIT Deemed to be University, Bhubaneswar, Odisha, India.

of 370 MHz, 380 MHz, and 1.4 GHz, respectively. A combination of the defected hexagonal patch with a semicircular patch loaded with a CSRR as a radiating element on one side and partial ground on the other side of the substrate was proposed [6] to operate in the resonant bands at 1.72/2.17 GHz with a bandwidth of 230 MHz in the first band and 420 MHz in the second band. It has a gain of 1.8 dB & 1.6 dB, respectively. A simple rectangular monopole antenna was proposed in [7] to resonate at 5.2 GHz. A second resonate frequency was produced at 4.1 GHz when an inverted L slot was etched on a monopole with the addition of single-cell metamaterial reactive loading. Then resonant frequency shifted down two wide bands from 2.3 GHz–4.1 GHz & 5 GHz–6.6 GHz.

A compact-size multiband monopole antenna with a CSRR was proposed in [8] with narrowband applications. To achieve triband, they introduced a single metamaterial loading along with a monopole antenna as proposed in [9]. In [11], a detailed metamaterial property extraction method was discussed along with equivalent circuit modeling of a unit cell. In the case of SRR, the metal part has the effect of inductance and the split gap has capacitance. Right-handed materials have series inductance & shunt capacitance, whereas left-handed materials have series capacitance and shunt inductance. [12] proposed a square-shaped single-slit resonator (SSR) and a modified hexagonal metal strip as an epsilon negative metamaterial with resonance at 2.89/9.42/15.16 GHz. [13] proposed a gap-coupled hexagonal SRR-based metamaterial for many applications in both the S and X bands. Left-handed materials can be categorized as double negative metamaterials and single negative metamaterials formed by SRR [14] at a certain frequency range.

In this paper, a monopole antenna with a single stub and two double-split ring resonators on either side of the feed line was considered as the radiating plane on one side & composite double-split ring resonators as the ground plane on the other side of the substrate. The antenna resonates at 3.38 GHz to 4.08 GHz and 4.64 GHz to 5.2 GHz, making it suitable for WLAN applications and satellite communication. A good bandwidth was achieved in these bands as compared to the literature. By increasing the number of stubs to four, these two bands have been merged into one single wideband, which ranges from 3.39 GHz to 5.13 GHz. A maximum gain of 3.3 dBi was observed with 47.93% bandwidth. There was a slight reduction in antenna size when DSRR/CDSRR unit cells were considered along with monopole antenna & gain also increased from 1.5 dBi to 3.3 dBi. Measured results were good in comparison with simulated values. The proposed antenna has improved parameters compared with existing antenna structures [5, 6, 16–18].

2. ANTENNA DESIGN

A monopole antenna with a stub was printed on one side of an FR-4 epoxy glass substrate ($0.4\lambda_0 \times 0.4\lambda_0 \times 0.021\lambda_0$) and a partial ground on the other side. The height of the substrate is taken as $0.021\lambda_0$, where λ_0 is the free space wavelength at the resonant frequency of 4 GHz. The proposed monopole antenna is simulated using ANSYS HFSS, whose top and bottom views are shown in Figure 1.

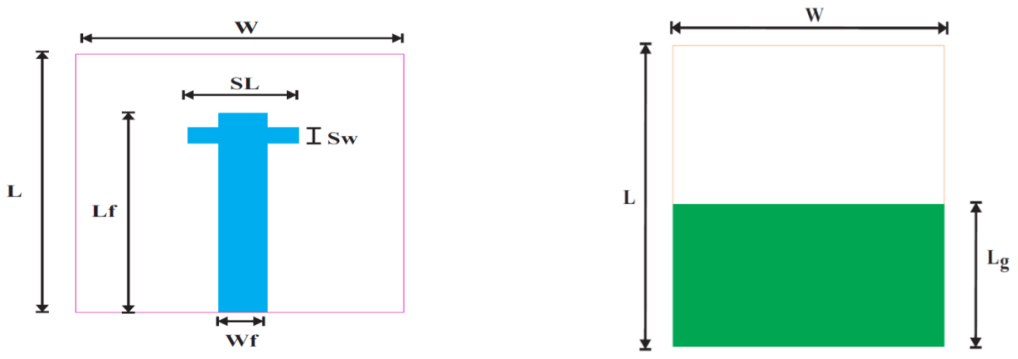

(a) Top View (b) Bottom View

Figure 1. Top and bottom view of proposed monopole antenna.

3. PARAMETRIC STUDY OF STUB BASED MONOPOLE ANTENNA

A detailed parametric study was carried out on the width of the monopole (Wf), length of the stub (SL), width of the stub (Sw), and length of the ground plane (Lg) to characterize antenna design, as shown in Figure 2. The optimized dimensions of the proposed monopole antenna with stubs are listed in Table 1.

Table 1. Optimized parameters of proposed monopole antenna with stubs.

Parameters	L	W	SL	Lf	Wf	Sw	Lg
Dimension in mm	30	30	10	25	4.4	2	15

From Figure 2(a), impedance matching improves with the width of the monopole. When the width increases, the resonant frequency increases, but there is a slight reduction in bandwidth. The reflection coefficient (S_{11}) was found to be below -10 dB from 3.55 GHz to 5.48 GHz, covering a bandwidth of 1.93 GHz with suitable impedance matching at 4.01 GHz for monopole width (Wf) at 4.4 mm. Impedance matching also depends on stub length. As length increases, so does the resonant frequency. At a resonant frequency of 4 GHz, the stub length (SL) is 10 mm, as shown in Figure 2(b).

As the width of the stub increases, the resonant frequency decreases. As the monopole antenna was designed to resonate at 4 GHz, a stub width (Sw) of 2 mm was chosen, as shown in Figure 2(c). The reflection coefficient also depends on the conventional ground; as the length of the ground increases, the impedance matching decreases, and there is a large shift in resonance frequency, as shown in Figure 2(d). The length of the monopole antenna above the ground plane must be nearly $0.25\lambda_0$ [15]. At 4 GHz,

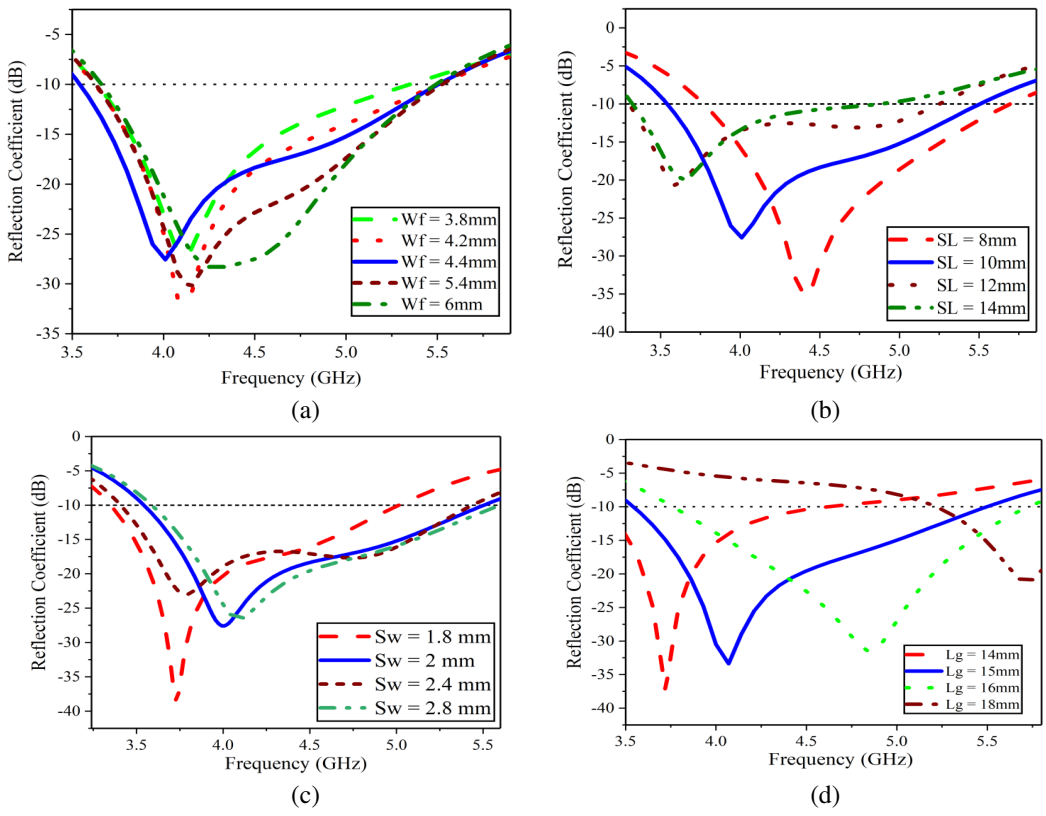

Figure 2. Parametric study of proposed antenna parameters. (a) Width of monopole. (b) Length of stub, (c) Width of stub. (d) Length of the ground.

the monopole length above the ground plane must be 18.75 mm. To minimize the antenna dimensions, the monopole antenna, along with stub size, was optimized as 18.2 mm. Optimized monopole antenna dimensions are given in Table 1.

4. ANTENNA DESIGN STEPS

1. Defined antenna material and the desired resonant frequency (Identified the design specifications by calculating the length of the monopole antenna as $L = \frac{\lambda}{4} = \frac{C}{4f_r}$, where $C = 3 \times 10^8$ m).
2. Determined the effective permittivity of the substrate

$$\varepsilon_{eff} = \frac{\varepsilon_r + 1}{2} + \frac{\varepsilon_r - 1}{2}\left[1 + 12\left(\frac{h}{W}\right)\right]^{-1/2}$$

   $\frac{w}{h} \gg 1$ where W = width of monopole & h = height of the substrate.
3. Specified the dimensions of the substrate & ground plane and simulated the antenna using HFSS.
4. Optimized antenna parameters like the width of the monopole, length of the stub, the width of the stub, and ground plane.
5. Fabrication was carried out after getting optimum values of antenna parameters using the Mits Eleven Lab PCB prototype machine.
6. Antenna measurement was carried out in an anechoic chamber. The distance between the transmitter & receiver was 1.5 meters. An Amkor horn antenna was considered for reference, whose operating range is 1 GHz to 18 GHz. An Agilent N5247A VNA was taken to measure the reflection coefficient.

5. METAMATERIAL UNIT CELL

A homogeneous artificial structure whose dimensions are in the order of a sub-wavelength of the resonance frequency is called a "metamaterial unit cell." These materials have unique properties like simultaneous negative permittivity and permeability in specific frequency ranges that cannot be found in natural materials. They are artificially formed periodic structures generally having copper strips as thin wires to obtain negative permittivity and split ring resonators to get negative permeability at any desired frequency. Metamaterials have unique properties like the reversal of Snell's law, the reversal of Cherenkov radiation, the reversed Doppler effect, and the negative refractive index. They found many applications in which electromagnetic waves were blocked or enhanced, absorbed or bent which conventional materials cannot do. As wave vectors, magnetic fields, and electric fields form a left-handed triplet, these materials are also called Left-Handed Materials (LHMs). In these materials, group & phase velocities are antiparallel, and they exhibit backward wave propagation. In single negative materials (SNMs), either electric permittivity or magnetic permeability is negative, whereas in double negative materials (DNMs), both electric permittivity & magnetic permeability are negative in the microwave or millimeter frequency range. There are two models for the characterization of the material properties; they are the Lorentz Model and Drude Model [11].

Metamaterial properties like permeability, permittivity, and refractive index can be obtained using many methods, and one such basic method is the Nicolson-Ross-Weir (NRW) method. The extracted relative permittivity, permeability, and refractive index can be expressed as

$$\begin{aligned} \varepsilon_r &\sim \frac{2}{jk_0 d} \times \frac{(1 - V_1)}{(1 + V_1)} \\ \mu_r &\sim \frac{2}{jk_0 d} \times \frac{(1 - V_2)}{(1 + V_2)} \\ \mu_r &= \sqrt{\varepsilon_r \mu_r} \end{aligned} \tag{1}$$

where $V_1 = |S_{11}| + |S_{21}|$, $V_2 = |S_{21}| - |S_{11}|$, d = substrate thickness, $k_0 = \frac{2\pi f}{c}$, c is the velocity of light, and d is the substrate thickness.

5.1. Proposed Metamaterial Unit Cell

As shown in Figure 3, a double split ring resonator (DSRR) shaped unit cell has been proposed. The dimensions of the unit cell ($0.17\lambda_0 \times 0.17\lambda_0 \times 0.02\lambda_0$) are in the order of sub-wavelength at the resonant frequency of 4 GHz. This unit cell was etched on FR-4 as a dielectric substrate with a thickness of 1.6 mm, having a permittivity of 4.4 and a loss tangent (δ) of 0.02.

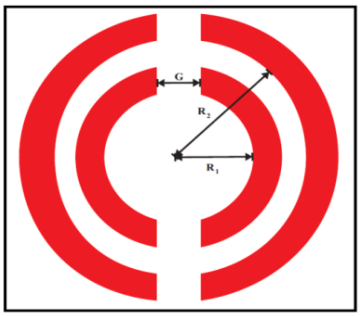

Figure 3. Top view of proposed double split ring resonator (DSRR).

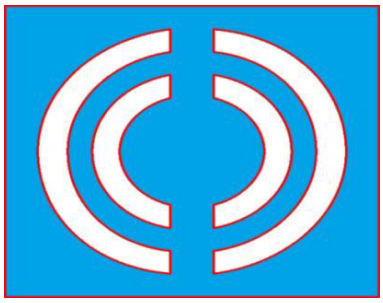

Figure 4. Top view of proposed complimentary double split ring resonator (CDSRR).

DSRR has been designed using the general sub-wavelength rule ($\lambda/10$) to resonate at 4 GHz. As the split gap produces parallel plate capacitance, and the metal strip has an inductance effect, this unit cell has negative permittivity & permeability at the resonance frequency of 3.4 GHz. By slightly varying the dimensions from $\lambda/10$ to $\lambda/13$ and introducing another split gap on the opposite side, the proposed unit cell behaves like a metamaterial from 3.3 GHz to 3.55 GHz and 4.25 GHz to 5.25 GHz, as shown in Figure 5. The inner (R_1) and outer (R_2) rings' radii are optimized to 3.5 mm and 5.5 mm, respectively. To have a uniform effect of inductance and capacitance, the width of each ring and the gap between the rings are considered to be 1 mm, whereas the split gap G is 1.5 mm. The proposed unit cell has been designed and simulated using 3D electromagnetic simulation software ANSYS HFSS as shown in Figure 3. In addition to the above-mentioned unit cell, two composite double split ring resonators (CDSRR) were considered to replace conventional ground, as shown in Figure 4.

Many methods for obtaining parameters such as electric permittivity and magnetic permeability have been presented in the literature. The most common method is the NRW method, in which

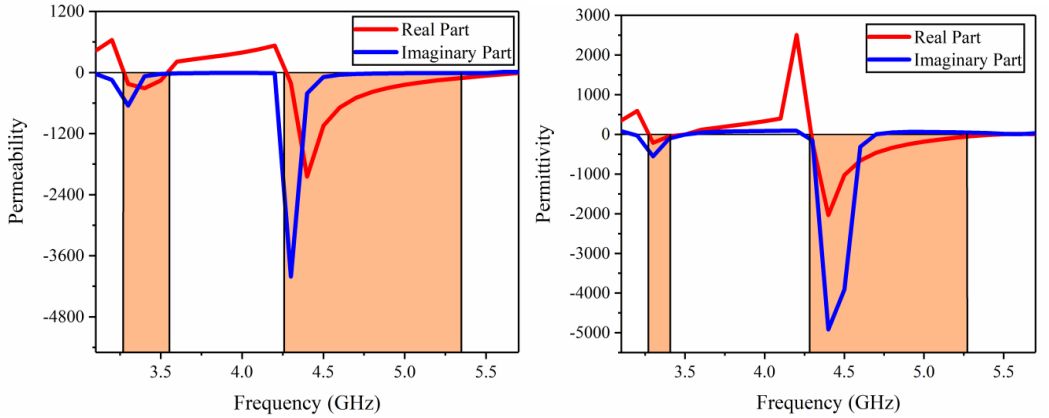

i. Permeability vs Frequency

ii. Permittivity vs Frequency

Figure 5. Electric permittivity & magnetic permeability of the proposed DSRR & CDSRR metamaterial unit cells.

transmission and reflection coefficient parameters of the unit cell for different frequencies were considered and substituted in equations [11] to extract metamaterial parameters like electric permittivity & magnetic permeability. These parameters are frequency dependent, and the OCTAVE code was generated using the above equations for which S_{11} & S_{21} of the unit cell are given as inputs and generate electric permittivity & magnetic permeability as outputs. Figure 5 shows the relationship between frequency and electric permittivity, and magnetic permeability.

Here, both real and imaginary parts of the proposed DSRR & CDSRR metamaterial unit cells exhibit negative values of permittivity & permeability in frequency ranges of 3.3 GHz to 3.55 GHz and 4.25 GHz to 5.25 GHz. It means that the proposed unit cells behaves as double negative materials in these two frequency bands.

When the resonant frequencies of the antenna & metamaterial unit cell are the same, incoming electromagnetic waves can either be transmitted or reflected. Here, the proposed monopole antenna with stubs has a reflection coefficient of below −10 dB in the frequency range from 3.6 GHz to 5.6 GHz, and the proposed DSRR unit cell behaves as DNMs at 4.25 GHz to 5.25 GHz. When these are combined, the incoming electromagnetic waves will either reflect or transmit due to which there is an improvement in antenna parameters.

- In conventional monopole antennas, the ground plane is generally a perfect electric conductor. *(Where incoming electromagnetic waves are antiparallel with reflected waves, and they cancel each other out).*
- In a metamaterial unit cell, due to its unique properties like negative permittivity & permeability, metamaterial will behave as artificial magnetic conductors *(Where incoming Electromagnetic waves are parallel with reflected waves).*

Due to good impedance matching, there is an improvement in reflection coefficient, bandwidth, and gain [14]. To further enhance the antenna performance, the conventional ground has been replaced by two CDSRR unit cells; these unit cells also have the characteristics as shown in Figure 5.

5.2. TL Model of Proposed Metamaterial Unit Cell

When an equivalent circuit model of the metamaterial unit cell was considered, the frequency at which resonance occurs is given as

$$f = \frac{1}{2\pi\sqrt{L_T C_T}} \tag{2}$$

where L_T is the total inductance (i.e., Self inductance (L_s), and mutual inductance (L_M)), and C_T is the total capacitance (i.e., parallel (C) and coplanar capacitance (C_{cp}))

$$L_s = 0.2\mu_0 \left(-\frac{w}{2}\sinh^{-1} 1 + \frac{w}{2}\sqrt{2} + \left(l - \frac{w}{2}\right)\sinh^{-1}\left(\frac{1-\frac{w}{2}}{\frac{w}{2}}\right) - \sqrt{\left(l-\frac{w}{2}\right)^2 + \left(\frac{w}{2}\right)^2}\right) \text{ H}$$

$$L_M = 0.2l \left(\ln\left(\frac{1}{d} + \sqrt{1+\frac{l^2}{d^2}}\right) - \sqrt{1+\frac{d^2}{l^2}} + \frac{d}{1}\right) \mu\text{H}$$

Coplanar capacitance is

$$C_{cp} = \frac{(\varepsilon_r + 1)\,\varepsilon_0}{2}\frac{1}{\pi}\ln\left[2\frac{1+\sqrt{k}}{1-\sqrt{k}}\right] \tag{3}$$

where $k = \sqrt{(1-(\frac{p}{p+2q})^2)}$, p = width of metal strips, q = distance between two metal strips. $C = \varepsilon(\frac{A}{d})$, where A is the area of metal strips.

The equivalent circuit model of the proposed metamaterial unit cell is shown in Figure 6. In the transmission line (TL) model, the metal strip has the effect of inductance, whereas the split gap acts as a capacitor. Two splits of the inner and outer rings along with two metal strips represent two parallel LC circuits where each branch has a series combination of inductor and capacitor. In Figure 6(a), the parallel LC circuit of the outer ring is formed by a series combination of L_1 and C_1 in one arm and a series combination of L_2 and C_2 in the other arm; the parallel LC circuit of the inner ring is formed

by a series combination of L_3 and C_3 in one arm and a series combination of L_4 and C_4 in the other arm; the parallel plate capacitance is formed by the split gap given as $C = \varepsilon(\frac{A}{d})$, where A is the area of metal strips, and co-planar capacitance is created between two rings. In the proposed unit cell, the width of the metal stripe (p) and the gap between two rings (q) is 1 mm.

The co-planar capacitance between two metal strips is 37.4 pF. The parallel combination of L_1C_1 & L_2C_2 controls the resonant frequency at 3.15 GHz where $L_T = 1.4$ nH (L_T is the total inductance, i.e., self-inductance and mutual inductance), and $C_T = 1.15$ pF (C_T is total capacitance, i.e., parallel and coplanar capacitance). Similarly, the parallel combination of L_3C_3 and L_4C_4 controls the resonant frequency at 4 GHz where $L_T = 1.25$ nH & $C_T = 1.26$ pF, and $C = 0.57$ pF is the parallel plate capacitance caused by dual splits. The above-discussed parameters have been studied by simulating equivalent circuits using ADS (Advanced Design System) software. The initial values of indicators and capacitors were calculated using the above equations. These values have been tuned to obtain a better magnitude of S_{21} & S_{11} of the proposed unit cell to match the resonant frequencies compared with results obtained by using HFSS software. In the case of a composite double split ring resonator, DSRR has been detached from metal. Figure 6(b) is the equivalent circuit where capacitance C is replaced by inductance L. Figure 7 shows the schematic view of the proposed unit cell as simulated in HFSS software. Wave port analysis was carried out for determining the transmission & reflection coefficient parameters of the unit cell to extract electric permittivity and magnetic permeability.

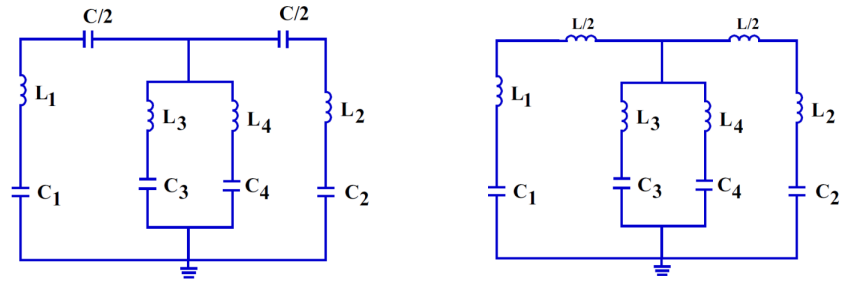

(a) Equivalent Circuit model of DSRR (b) Equivalent Circuit Model of CDSRR

Figure 6. Transmission line (TL) model of the proposed metamaterial unit cells.

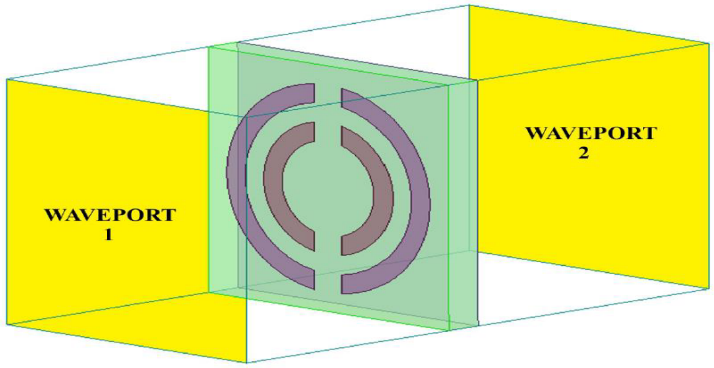

Figure 7. Schematic view of metamaterial unit cell simulated in HFSS software.

6. PARAMETRIC STUDY OF PROPOSED METAMATERIAL BASED MONOPOLE ANTENNA

Four different antenna structures are proposed to study the effect of stubs and metamaterial unit cells on monopole antenna parameters. Antenna1 was designed by placing two proposed DSRR unit cells along the feed of a monopole antenna and replacing conventional ground with a CDSRR unit cell.

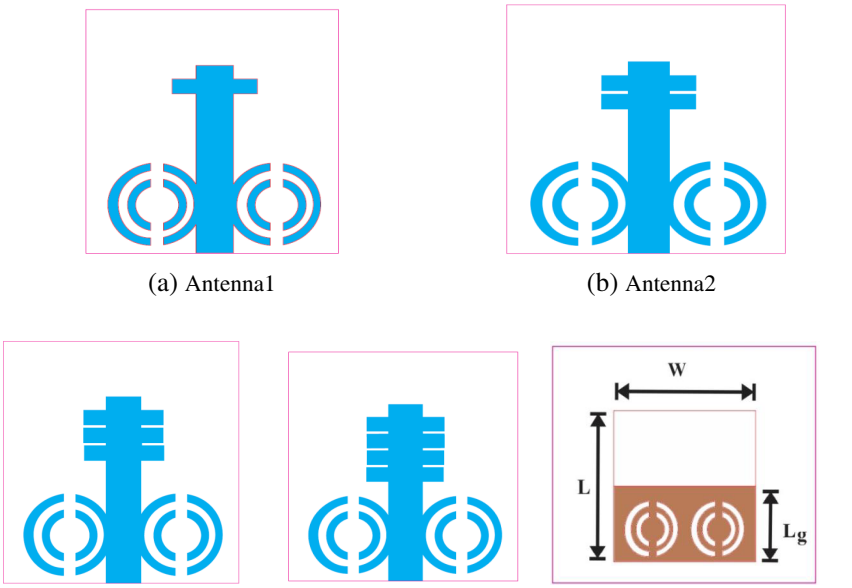

(a) Antenna1 (b) Antenna2

(c) Antenna3 (d) Antenna4 (e) CDSRR unit cell Ground Plane

Figure 8. Proposed four antenna designs along with CDSRR unit cell ground plane.

The position of these unit cells was optimized to achieve better impedance bandwidth in the desired frequency range. In Antenna2, another stub is added by optimizing the space between stubs to be 0.4 mm for better coupling. Furthermore, another stub was included to get Antenna3, and finally, a fourth stub was added to form Antenna4 structure. In all these structures, CDSRR unit cells were considered in the ground plane, as shown in Figure 8. The width of the monopole has been optimized by a parametric study to match 50 Ω line and SMA connector.

A detailed analysis was carried out, and Antenna4 structure has been fabricated using an FR4 substrate with a relative permittivity of 4.4 and loss tangent of 0.02. Two composite double split ring resonators have been detached on one side & double split ring resonators along with monopole feed on the other side as shown in Figure 9.

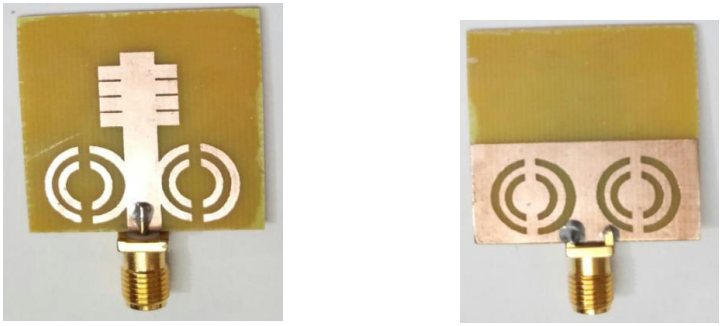

(a) Top View (b) Bottom View

Figure 9. Fabricated prototype of proposed Antenna4 structure.

7. RESULTS AND DISCUSSIONS

The proposed antennas were printed on one side of the FR-4 substrate, whose dielectric constant is 4.4 with thickness of 1.6 mm, and on the other side, CDSRR unit cells simulated these antenna structures using 3D electromagnetic simulator HFSS software. The antenna was designed in four steps as Antenna1

consists of a single stub, and a DSRR unit cell loaded monopole antenna was designed and simulated whose dimensions were optimized for proper impedance matching with 50 Ω line as given in Table 1. A reflection coefficient below −10 dB was observed in the frequency range 3.38 GHz to 4.08 GHz with a maximum of −31.67 dB at 3.59 GHz having a bandwidth of 700 MHz & 4.64 GHz to 5.2 GHz and with a maximum of −35 dB at 4.78 GHz having a bandwidth of 560 MHz. Further, to improve the operating frequency band, another stub was included in Antenna1 with an optimized gap between the two stubs of 0.4 mm to get Antenna2 structure. A reflection coefficient below −10 dB was observed in the frequency range 3.31 GHz to 4.08 GHz with a maximum of −27.86 dB at 3.52 GHz having a bandwidth of 770 MHz & 4.57 GHz to 5.34 GHz and with a maximum of −30.54 dB at 4.92 GHz having a bandwidth of 770 MHz. Though there was a slight reduction in the reflection coefficient, there was a slight improvement of 70 MHz bandwidth in the first band, and a good improvement of 210 MHz bandwidth in the second band was noticed in Antenna2. When another stub was included with the same gap of 0.4 mm between all stubs to get the Antenna3 structure, a reflection coefficient below −10 dB was observed in the frequency range 3.38 GHz to 4.08 GHz with a maximum of −22.57 dB at 3.52 GHz having a bandwidth of 700 MHz & 4.36 GHz to 5.2 GHz with a maximum of −17.78 dB at 4.92 GHz having a bandwidth of 840 MHz. The effect of stubs in the first band is less than the second band. As the number of stubs increased, there was a good improvement in the bandwidth of the second band with only a slight variation in the first band. When the fourth stub was included in Antenna4 structure, a reflection coefficient below −10 dB was achieved in the frequency range of 3.39 GHz to 5.13 GHz with a maximum of 28.98 dB at 3.63 GHz having a bandwidth of 1740 MHz. Simulated results for different proposed antenna structures are shown in Figure 10.

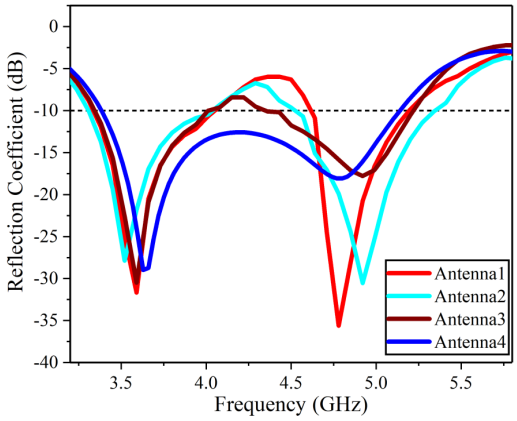

Figure 10. Reflection coefficient verses frequency for different proposed antenna structures.

As the number of stubs increased, the coupling effect between them improved the impedance matching due to which two smaller bands were merged. As shown in Figure 10, Antenna4 has a single wideband, i.e., the two bands of three antenna structures were merged to get a single wideband, making it suitable for WLAN, Wi-Fi, and WiMAX.

Figure 11 shows the radiation pattern of the proposed antenna structure for both E-plane and H-plane. Here the patterns are the same for all antenna structures, i.e., they are bidirectional radiation patterns (double dumbbell shape) in the E-plane and omnidirectional radiation patterns (circular) in the H-plane except for Antenna1 structure. The maximum gain for all the proposed antenna structures is 3.3 dBi, and it is nearly constant in the desired frequency range. Figure 12 shows the gain pattern in the desired frequency range of all the proposed antenna structures. Gain is flat and the same for all the proposed antenna structures, and it falls outside the desired frequency range.

Antenna4 structure has been fabricated, and the reflection coefficient has been measured using VNA Agilent N5247A: A.09.90.02. The gain and radiation patterns for both E-plane and H-plane have been measured in an anechoic chamber, as shown in Figure 13.

When being measured with a Vector Network Analyzer, Antenna4 structure has a reflection

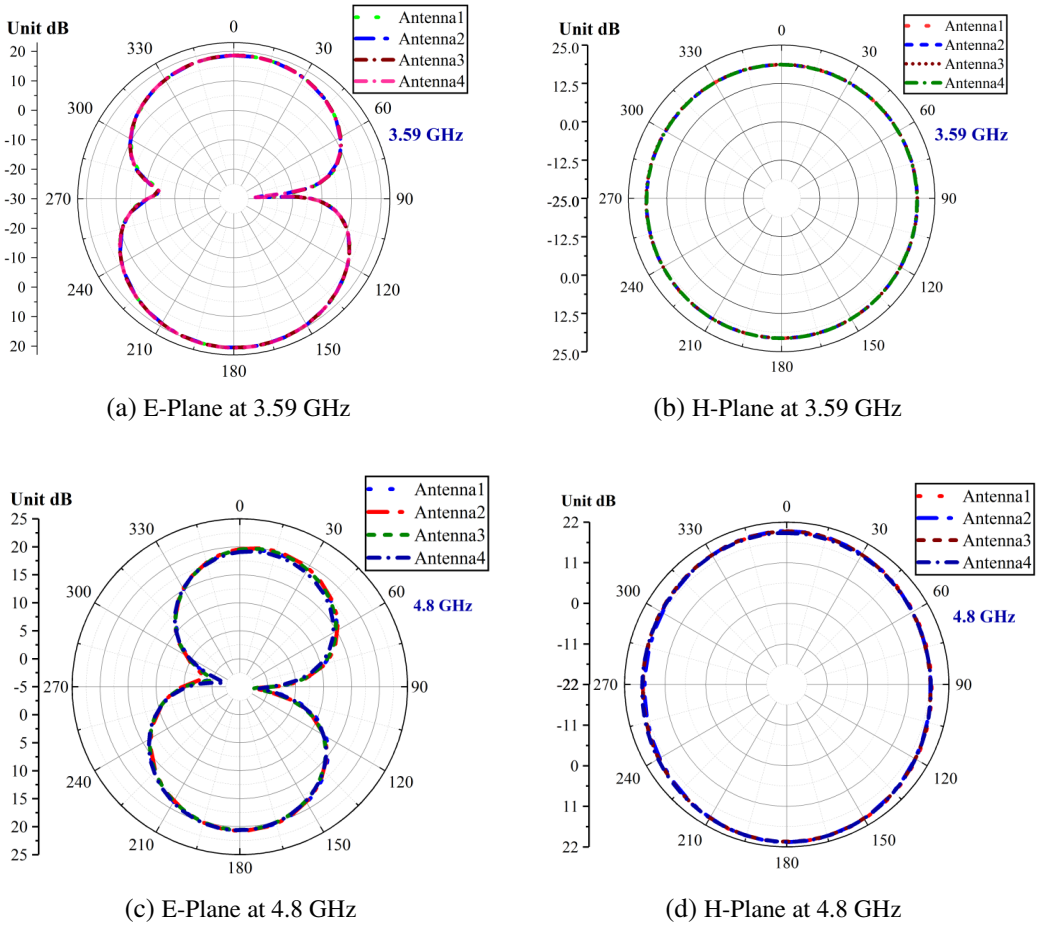

(a) E-Plane at 3.59 GHz (b) H-Plane at 3.59 GHz

(c) E-Plane at 4.8 GHz (d) H-Plane at 4.8 GHz

Figure 11. Radiation pattern of proposed antenna structures.

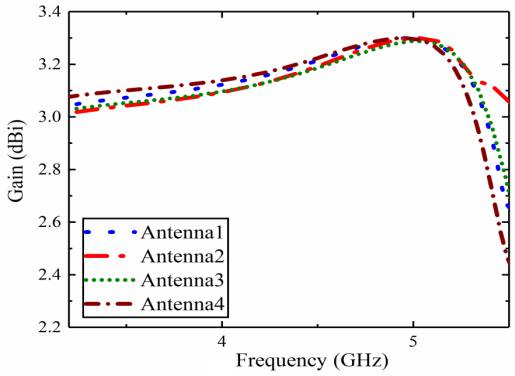

Figure 12. Gain pattern.

coefficient of less than −10 dB in the frequency range of 3.25 GHz to 5.30 GHz, with a maximum value of −44.93 dB at 3.54 GHz and a bandwidth of 2045 MHz. Figure 14(a) shows that bandwidth has been improved by 305 MHz compared to simulated results, a nearly 10% improvement. Figures 14(b) and 14(c) show that the gain pattern and radiation were the same for both measured and simulated values.

Compared to the stub monopole with a conventional ground plane, placing metamaterial unit cells along the monopole feed line and in the ground plane improved the impedance bandwidth and reflection coefficient as shown in Figure 15. Antenna miniaturization has been improved from $0.4\lambda_0$ to $0.36\lambda_0$,

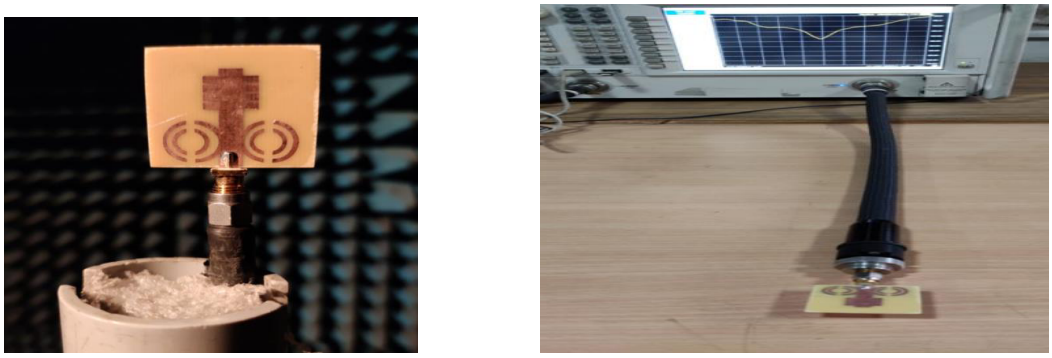

(a) Measured radiation pattern & Gain (b) Determining Reflection Coefficient

Figure 13. Testing Antenna4 in an anechoic chamber & using VNA.

where λ_0 is the free space wavelength at the resonant frequency of 4 GHz.

Referring to Figure 1(a), though the B.W. is almost the same as the DSRR resonator, there is a good improvement in the gain of Antenna4 as shown in Figure 16. The above graph shows frequency versus antenna efficiency. Here, antenna efficiency (η) is more than 90% in the desired frequency range. The current distribution of different proposed antenna structures is shown in Figure 17. The feed line of the monopole antenna carried out maximum radiation, and it radiates omnidirectionally in the E-plane and uniformly in the H-plane, resembling a similar pattern as in the case of an ideal monopole antenna at 3.59 GHz frequency with maximum radiation at 0 degrees, as shown in Figs. 11(a) and 11(b), but there is a slight deviation in the E-plane at 4.8 GHz as shown in Fig. 11(c). Maximum radiation has been carried by the monopole feed line, stub, and CDSRR unit cell loaded ground plane, as shown in Figure 17(a).

There was a good coupling between DSRR & CDSRR, and incoming electromagnetic waves were reflected from the ground plane, improving antenna parameters. As shown in Figure 17(b), there were a good coupling between the stubs and an increase in bandwidth. As the number of stubs increased, there was an improvement in bandwidth. For Antenna4 structure, two small bands of Antenna3 were merged into a single band, and bandwidth has been improved to 2045 MHz (measured value). As shown in Figure 17(e), the CDSRR unit cells in the passive ground plane were coupled with DSRR unit cells and the monopole.

Table 2. Comparison of proposed antenna with existing antennas described in literature.

Ref.	**Size (mm^2)**	**Bands Covered (GHz)**	**Bandwidth (MHz)**	**Gain (dBi)**	**Metamaterial Unit Cell**	
					Equivalent Circuit Analysis	**Verification of metamaterial property**
[5]	48×48	1.9/2.45/5	370/380/1480	1.64/2.07/4.06	Not Computed	Verified
[6]	50×50	1.72/2.17	230/420	1.8/1.6	Not Computed	Not Verified
[16]	122×60	0.9/2	140/460	0/06/2.2	Computed	Not Verified
[17]	34×30	2.4/3.3/5.2	440/200/200	-1/1/4	Not Computed	Not Verified
[18]	40×50	1.65/1.93/2.2	69.9/60/280	1.08/1.82/2.93	Not Computed	Not Verified
[20]	55×54.5	1.8/3.5	166/802	2.6/2.59	Computed	Not Verified
[21]	28×20	2.2/2.7/5.4	210/400/440	2.4/2.37/5.5	Computed	Not Verified
[22]	21×29	24/3.4/5.1/5.8	218/389/190/270	NA	Not Computed	Not Verified
Proposed	$\mathbf{30 \times 30}$	**3.25 to 5.29**	**2045**	**3.3**	**Computed**	**Verified**

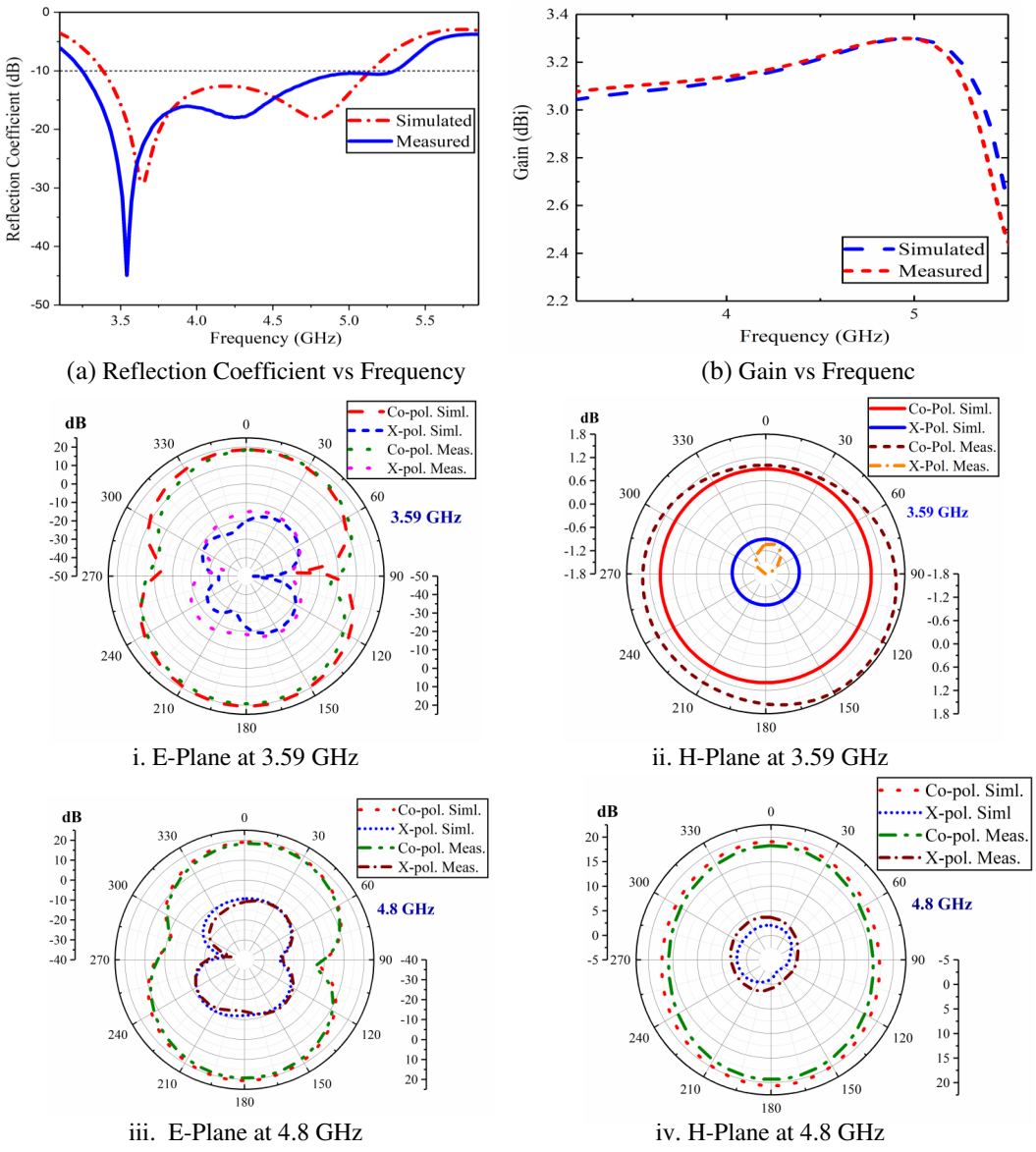

(a) Reflection Coefficient vs Frequency

(b) Gain vs Frequenc

i. E-Plane at 3.59 GHz

ii. H-Plane at 3.59 GHz

iii. E-Plane at 4.8 GHz

iv. H-Plane at 4.8 GHz

(c) Radiation Pattern for both E-Plane & H-Plane

Figure 14. Measured & simulated results of Antenna4 structure.

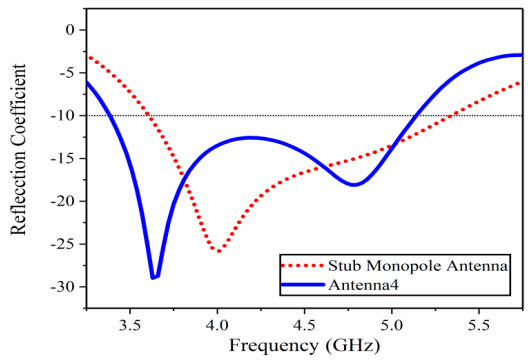

Figure 15. Reflection coefficient of stub monopole antenna & Antenna4.

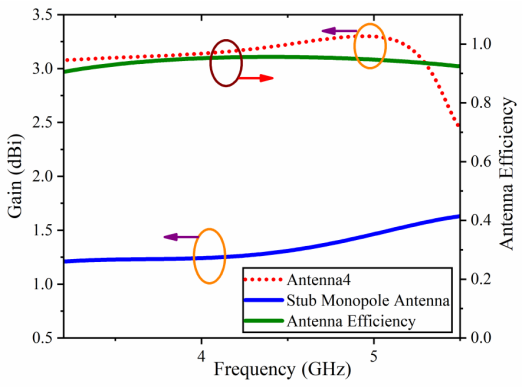

Figure 16. Gain and efficiency of Antenna4 (proposed) along with stub monopole antenna.

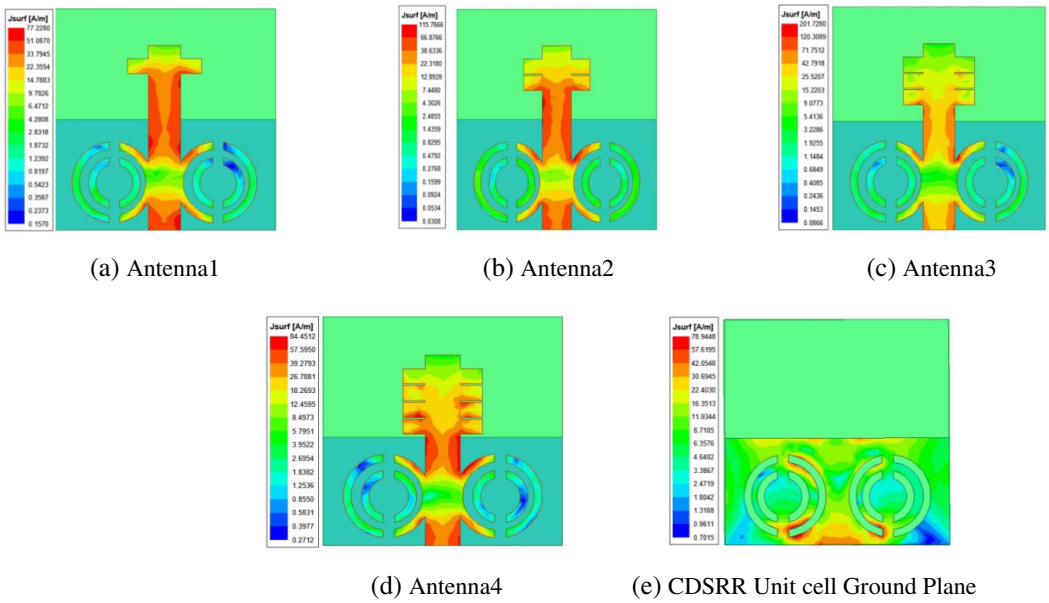

(a) Antenna1 (b) Antenna2 (c) Antenna3

(d) Antenna4 (e) CDSRR Unit cell Ground Plane

Figure 17. Current distribution for different proposed antenna structures.

From Table 2, the proposed antenna has features like compact size, wide band from 3.25 GHz to 5.29 GHz, and improved gain. However, existing antennas have multi-bands with narrow bandwidth. The proposed antenna has dual-bands when the number of stubs is less than or equal to three, but has a good bandwidth compared with literature. For wideband, four stubs were considered. Measured results are in good comparison with simulated ones.

8. CONCLUSION

A monopole antenna loaded with a DSRR with a feed line and two CDSRR unit cells in the ground plane was designed. When a single stub was considered in Antenna1 design, dual resonant bands were achieved at 3.38 GHz to 4.08 GHz and 4.64 GHz to 5.2 GHz, having a bandwidth of 700 MHz and 560 MHz, respectively. When another stub was added as in Antenna2, then there was no significant effect in the first band, but the second band has an improvement of 210 MHz bandwidth. Furthermore, when four stubs were added as in Antenna4, previous bands merged to form a single wideband with a bandwidth of 57.93% and a bandwidth of 2045 MHz (measured value). Gain also increased from 1.5 dBi to 3.3 dBi when DSRR/CDSRR unit cells were considered along with a monopole antenna, and there

was a slight reduction in antenna size. By increasing the number of stubs, two closely spaced narrow bands can be merged into a single wideband. The proposed antenna can be used for wireless applications like WLAN, WiFi, WiMAX [19–22], fixed satellite communication (space to earth and earth to space) aeronautical mobile, aeronautical radio navigation, and radio navigation-satellite (space to earth, space to space). Many devices have multiple antennas to operate in antenna bands that are closely spaced. In the proposed Antenna4 closely spaced multi-bands can be merged into a single wideband, making it suitable for the use for multi-devices. If isolation is required, we can reduce the number of stubs from four to either three or two.

REFERENCES

1. Wang, K., E. Kedze, and I. Park, "A high-gain and wideband series-fed angled printed dipole array antenna," *IEEE Transactions on Antennas and Propagation*, Vol. 68, No. 7, 5708–5713, Jul. 2020.
2. Wong, K., H. Chang, C. Wang, and S. Wang, "Very-low-profile grounded coplanar waveguide-fed dual-band WLAN slot antenna for on-body antenna application," *IEEE Antennas and Wireless Propagation Letters*, Vol. 19, No. 1, 213–217, Jan. 2020.
3. Wang, Z., J. Liu, and Y. Long, "A simple wide-bandwidth and high-gain microstrip patch antenna with both sides shorted," *IEEE Antennas and Wireless Propagation Letters*, Vol. 18, No. 6, 1144–1148, Jun. 2019.
4. Samson Daniel, R., R. Pandeeswari, and S. Raghavan, "A compact metamaterial loaded monopole antenna with offset-fed microstrip line for wireless applications," *AEU-International Journal of Electronics and Communications*, Vol. 83, 88–94, 2018.
5. Alam, T., M. Samsuzzaman, M. R. I. Faruque, and M. T. Islam, "A metamaterial unit cell inspired antenna for mobile wireless applications," *Microwave and Optical Technology Letters*, Vol. 58, 263–267, 2016.
6. Sharma, S. K. and R. K. Chaudhary, "Dual-band metamaterial-inspired antenna for mobile applications," *Microwave and Optical Technology Letters*, Vol. 57, 1444–1447, 2015.
7. Huang, H., Y. Liu, S. Zhang, and S. Gong, "Multiband metamaterial-loaded monopole antenna for WLAN/WiMAX applications," *IEEE Antennas and Wireless Propagation Letters*, Vol. 14, 662–665, 2015.
8. Behera, P. and S. S. Behera, "Compact multiband monopole antenna with complementary split ring resonator for WLAN and WIMAX applications," *NCRAEEE Conference Proceedings, International Journal of Engineering & Technology (IJERT)*, 2015.
9. Zhu, J., M. A. Antoniades, and G. V. Eleftheriades, "A compact tri-band monopole antenna with single-cell metamaterial loading," *IEEE Transactions on Antennas and Propagation*, Vol. 58, No. 4, 1031–1038, Apr. 2010.
10. Cao, F., S. W. Cheung, and T. I. Yuk, "A multi-band slot antenna for GPS/WiMAX/WLAN systems," *IEEE Transactions on Antennas and Propagations*, Vol. 63, 952–958, Mar. 2015.
11. Moniruzzaman, M., M. T. Islam, N. Misran, et al., "Inductively tuned modified split ring resonator based quad band epsilon negative (ENG) with near zero index (NZI) metamaterial for multiband antenna performance enhancement," *Sci. Rep.*, Vol. 11, 11950, 2021.
12. Afsar, S. U., M. R. I. Faruque, M. J. Hossain, M. U. Khandaker, H. Osman, and S. Alamri, "Modified Hexagonal split ring resonator based on an epsilon-negative metamaterial for triple-band satellite communication," *Micromachines*, Vol. 12, 878, 2021.
13. Shahidul Islam, M., M. Samsuzzaman, G. K. Beng, N. Misran, N. Amin, and M. T. Islam, "A gap coupled hexagonal split ring resonator based metamaterial for S-band and X-band microwave applications," *IEEE Access*, Vol. 8, No. 8, 68239–68253, 2020.
14. Islam, M. R., M. Samsuzzaman, N. Misran, G. K. Beng, and M. T. Islam, "A tri-band left-handed meta-atom enabled designed with a high effective medium ratio for microwave-based applications," *Results Phys.*, Vol. 17, 103032, Jun. 2020.
15. Balanis, C., *Antenna Theory, Analysis, and Design*, 2nd Edition, Wiley, New York, 1997.

16. Li, L., Z. Jia, F. Huo, and W. Han, "A novel compact multiband antenna employing dual-band CRLH-TL for smart mobile phone application," *IEEE Antennas and Wireless Propagation Letters*, Vol. 12, 1688–1691, 2013
17. Basaran, S., U. Olgun, and K. Sertel, "Multiband monopole antenna with complementary split-ring resonators for WLAN and WiMAX applications," *Electron. Lett.*, Vol. 49, 636–638, 2013.
18. Sarkar, D., K. Saurav, and K. Srivastava, "Multi-band microstrip-fed slot antenna loaded with a split-ring resonator," *Electron. Lett.*, Vol. 50, 1498–1500, 2014.
19. Behera, S. S. and S. Sahu, "Frequency reconfigurable antenna inspired by metamaterial for WLAN and WiMAX application," *2014 International Conference on Signal Propagation and Computer Technology (ICSPCT 2014)*, 442–446, 2014.
20. Dakhli, N. and F. Choubani, "Dual band metamaterial inverted-L antenna," *2019 IEEE 19th Mediterranean Microwave Symposium (MMS)*, 1–4, 2019.
21. Mishra, A., M. Ameen, and R. K. Chaudhary, "A compact triple band metamaterial inspired antenna using SRR and Hexagonal stub for UMTS, WLAN, and WiMAX applications in S/C bands," *2019 URSI Asia-Pacific Radio Science Conference (AP-RASC)*, 1–4, 2019.
22. Thankachan, S. and B. Paul, "A compact metamaterial inspired CPW fed multiband monopole antenna for wireless applications," *2020 IEEE International Symposium on Antennas and Propagation and North American Radio Science Meeting*, 427–428, 2020.